

SLAC-145  
UC-34  
(EXP)

MEASUREMENT OF THE DECAY  $K_L^0 \rightarrow \pi^0 \pi^0$  \*

G. AKAVIA,\*\* R. COOMBES, D. DORFAN,\*\*\* J. ENSTROM,  
D. FRYBERGER, R. PICCIONI, D. PORAT, D. RAYMOND,† K. RILEY,††  
A. ROTHENBERG, H. SAAL, M. SCHWARTZ, and S. WOJCICKI†††

STANFORD LINEAR ACCELERATOR CENTER  
and  
PHYSICS DEPARTMENT  
STANFORD UNIVERSITY  
Stanford, California 94305

PREPARED FOR THE U. S. ATOMIC ENERGY  
COMMISSION UNDER CONTRACT NO. AT(04-3)-515

April 1972

Printed in the United States of America. Available from National Technical Information Service, U. S. Department of Commerce, 5285 Port Royal Road, Springfield, Virginia 22151. Price: Printed Copy \$3.00; microfiche \$0.95.

- 
- \*Work supported in part by the U. S. Atomic Energy Commission and the U. S. Air Force Office of Scientific Research, Contract No. F44620-67-C-0070.  
\*\*Present address: Weizmann Institute of Science, Rehovoth, Israel.  
\*\*\*Present address: University of California, Santa Cruz, California;  
Alfred P. Sloan Foundation Fellow.  
†Present address: University of Hawaii, Hilo, Hawaii.  
††Present address: Cambridge University, Cambridge, England.  
†††Alfred P. Sloan Foundation Fellow.

## ABSTRACT

A measurement of the rate  $\Gamma(K_L^0 \rightarrow 2\pi^0)$  has been made relative to the rates  $\Gamma(K_L^0 \rightarrow 3\pi^0)$ ,  $\Gamma(K_L^0 \rightarrow \pi^\pm \mu^\mp \bar{\nu}_\mu)$  and  $\Gamma(K_L^0 \rightarrow \pi^\pm e^\mp \bar{\nu}_e)$  in a spark chamber scintillation counter experiment. Using published branching rates of the three body decays relative to the rate  $\Gamma(K_L^0 \rightarrow \text{all})$  and the rate  $\Gamma(K_S^0 \rightarrow 2\pi^0)$  we get  $\Gamma(K_L^0 \rightarrow 2\pi^0)/\Gamma(K_L^0 \rightarrow 3\pi^0) = 3.2 \pm 2.5 \times 10^{-3}$  and the CP violation parameter  $|\eta_{00}|^2 = 3.6 \pm 2.9 \times 10^{-6}$ . This is in agreement with the previous average for  $|\eta_{00}|$ .

## ACKNOWLEDGMENTS

Many people worked for many years on this project. Karl Hense, Dale Ouimette and Don Clark built and maintained much of the equipment. George Ike and Jeff Hobson measured all of the events. The Stanford Linear Accelerator Center and its staff carried out an obviously essential role.

## TABLE OF CONTENTS

	Page
Introduction . . . . .	1
Apparatus . . . . .	2
Operation . . . . .	9
Data Reduction . . . . .	10
Normalization . . . . .	15
Regenerator Analysis . . . . .	17
Pi-Pi Opening Angle Analysis . . . . .	20
Results . . . . .	28

## LIST OF TABLES

		Page
1.	Normalization . . . . .	16
2.	Regenerator $2\pi^0$ Analysis . . . . .	21

## LIST OF FIGURES

1.	K <sub>L</sub> <sup>0</sup> beam lines. . . . .	3
2.	K <sub>L</sub> <sup>0</sup> momentum spectrum at target. . . . .	4
3.	Detection apparatus (collimation for first data run). . . . .	6
4.	Perspective view of detection apparatus (collimation for second data run). . . . .	7
5.	Difference between corrected triplet times for good 3-6 $\gamma$ events from first data run. . . . .	13
6.	Time-of-flight for 3-6 $\gamma$ events. . . . .	14
7.	K <sub>L</sub> <sup>0</sup> mass for 4 $\gamma$ regenerator, (a) unlatched (b) latched. . . . .	19
8.	$\cos \theta_{\pi\pi}$ for 4 $\gamma$ regenerator, unlatched. . . . .	22
9.	$\cos \theta_{\pi\pi}$ for 4 $\gamma$ regenerator with kinematical cuts, unlatched. . . . .	23
10.	$\cos \theta_{\pi\pi}$ for normal running 4 $\gamma$ , latched and unlatched. . . . .	25
11.	$\cos \theta_{\pi\pi}$ for normal running 4 $\gamma$ with kinematical cuts (a) unlatched (b) latched. . . . .	26

## INTRODUCTION

This paper presents the results of an experiment to measure the branching ratio  $\Gamma(K_L^0 \rightarrow 2\pi^0)/\Gamma(K_L^0 \rightarrow 3\pi^0)$ . Knowledge of the characteristics of the decays  $K_L^0 \rightarrow 2\pi^0$  and  $K_L^0 \rightarrow \pi^+\pi^-$  is necessary for an understanding of the CP-violation exhibited by the  $K^0-\bar{K}^0$  system.<sup>1</sup> If we write the two physical eigenstates as

$$|K_S\rangle = [(|K^0\rangle + |\bar{K}^0\rangle) + \epsilon(|K^0\rangle - |\bar{K}^0\rangle)] / \sqrt{2(1 + |\epsilon|^2)}$$

$$|K_L\rangle = [(|K^0\rangle - |\bar{K}^0\rangle) + \epsilon'(|K^0\rangle + |\bar{K}^0\rangle)] / \sqrt{2(1 + |\epsilon'|^2)}$$

then

$$\eta_{+-} = \frac{\langle \pi^+\pi^- | H | K_L \rangle}{\langle \pi^+\pi^- | H | K_S \rangle} = \epsilon + \epsilon'$$

$$\eta_{00} = \frac{\langle \pi^0\pi^0 | H | K_L \rangle}{\langle \pi^0\pi^0 | H | K_S \rangle} = \epsilon - 2\epsilon'$$

where H is the interaction Hamiltonian and  $\epsilon' = \frac{i}{\sqrt{2}} \frac{\text{Im}(A_2)}{A_0} e^{i(\delta_2 - \delta_0)}$  with  $A_I e^{i\delta_I} = \langle K^0 | H | (2\pi)_I \rangle$  with  $\delta_I$  the pion phase shifts and I being the isospin of the  $2\pi$  state.

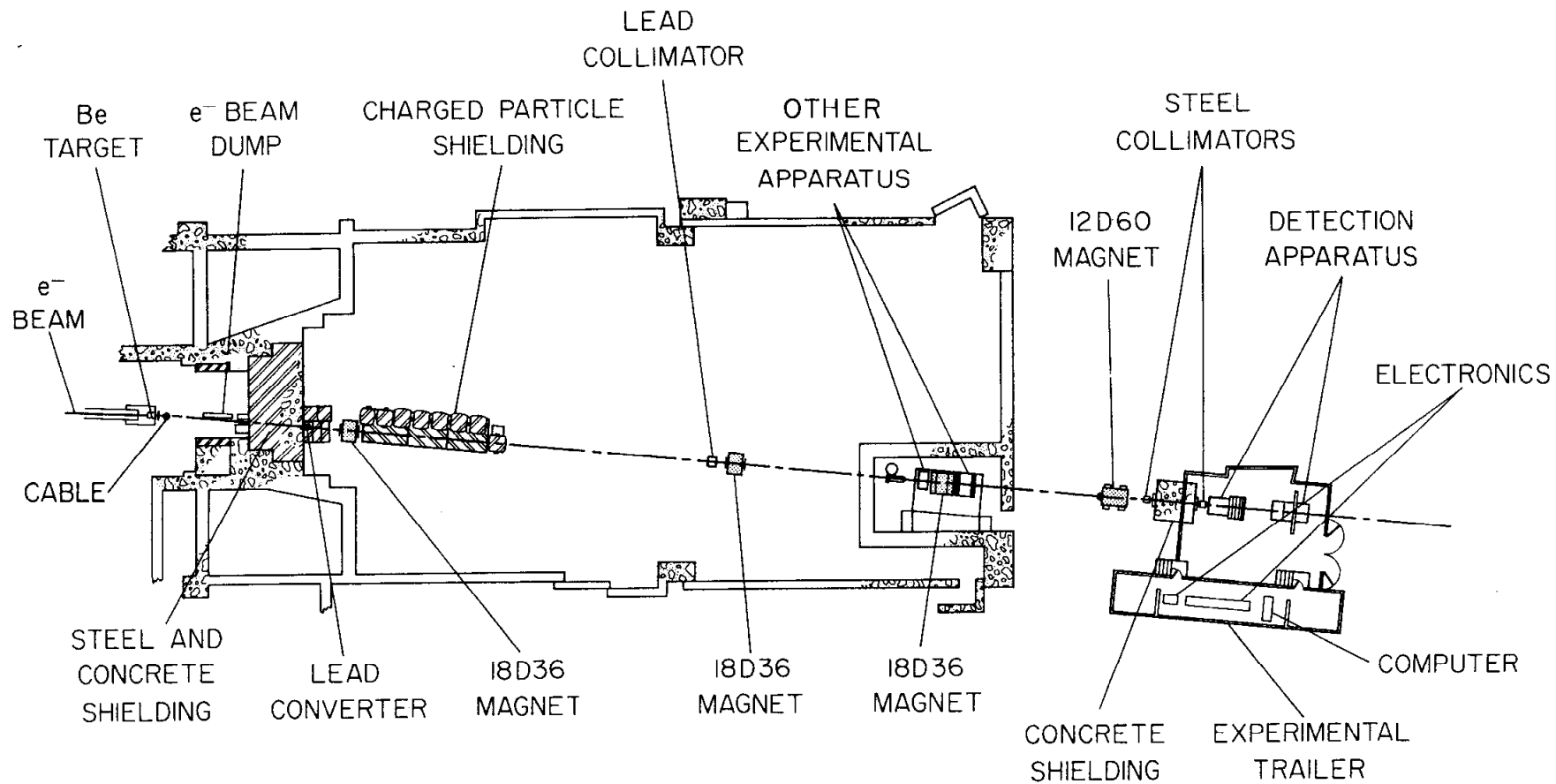
Our experiment determines  $|\eta_{00}|^2$  when combined with the experimental data for  $\Gamma(K_L^0 \rightarrow 3\pi^0)$  and  $\Gamma(K_S^0 \rightarrow \pi^0\pi^0)$ . A previously published portion of the present experiment measured  $\Gamma(K_L^0 \rightarrow 2\gamma)/\Gamma(K_L^0 \rightarrow \text{all})$ .<sup>2</sup>

Efficient detection of gamma rays and the separation of the  $K_L^0 \rightarrow 2\pi^0$  decays from the more common  $K_L^0 \rightarrow 3\pi^0$  decays are the main problems in the experiment. The mean energy of our  $K_L$  beam was high enough so that most of the

gammas were moving forward. This meant that a single spark chamber oriented perpendicular to the beam would have a high geometric efficiency. Making this chamber out of aluminum meant that high energy gamma showers had a considerable range and also that the showers formed a narrow cone, thus giving both the energy and the direction of the shower. Another major advantage of the beam was its time structure<sup>3</sup> which allowed us to do time-of-flight measurements on the incident particles. This gave us the energy of a decaying  $K_L^0$  and also helped eliminate background from neutron interactions.

### APPARATUS

The experiment was done at SLAC. A neutral beam was generated from a beryllium target at  $3^\circ$  to the incident 16 GeV electron beam (see Fig. 1). After passing through 10-18 inches of lead to remove gammas and approximately 80 meters of air, collimators and sweeping magnets it entered our apparatus. The final collimation defined the beam to 1 inch vertical and either 6 or 1 inch horizontal (for different portions of the experiment). A beam "knockout" system gave us a time structure of one rf bunch every 50 nsec. Each bunch had an inherent length of  $\frac{1}{100}$  nsec at the target. A probe in the electron beam just after the target provided a "cable" pulse, a time reference for the time-of-flight measurement. It also allowed us to monitor the time structure with a sampling scope. We normally ran 180 pulses/sec and 30 bunches/1.5  $\mu$ sec pulse. As the beam entered the detector it consisted of a roughly equal mixture of  $K_L^0$  and neutrons with most of the latter having momenta below 1 GeV/c and arriving after the kaons. The  $K_L^0$  spectrum of this beam was known from an earlier bubble chamber experiment by Brody et al.,<sup>4</sup> and is shown in Fig. 2.



- 3 -

1668C2

END STATION B

FIG. 1--K<sub>L</sub><sup>0</sup> beam line.



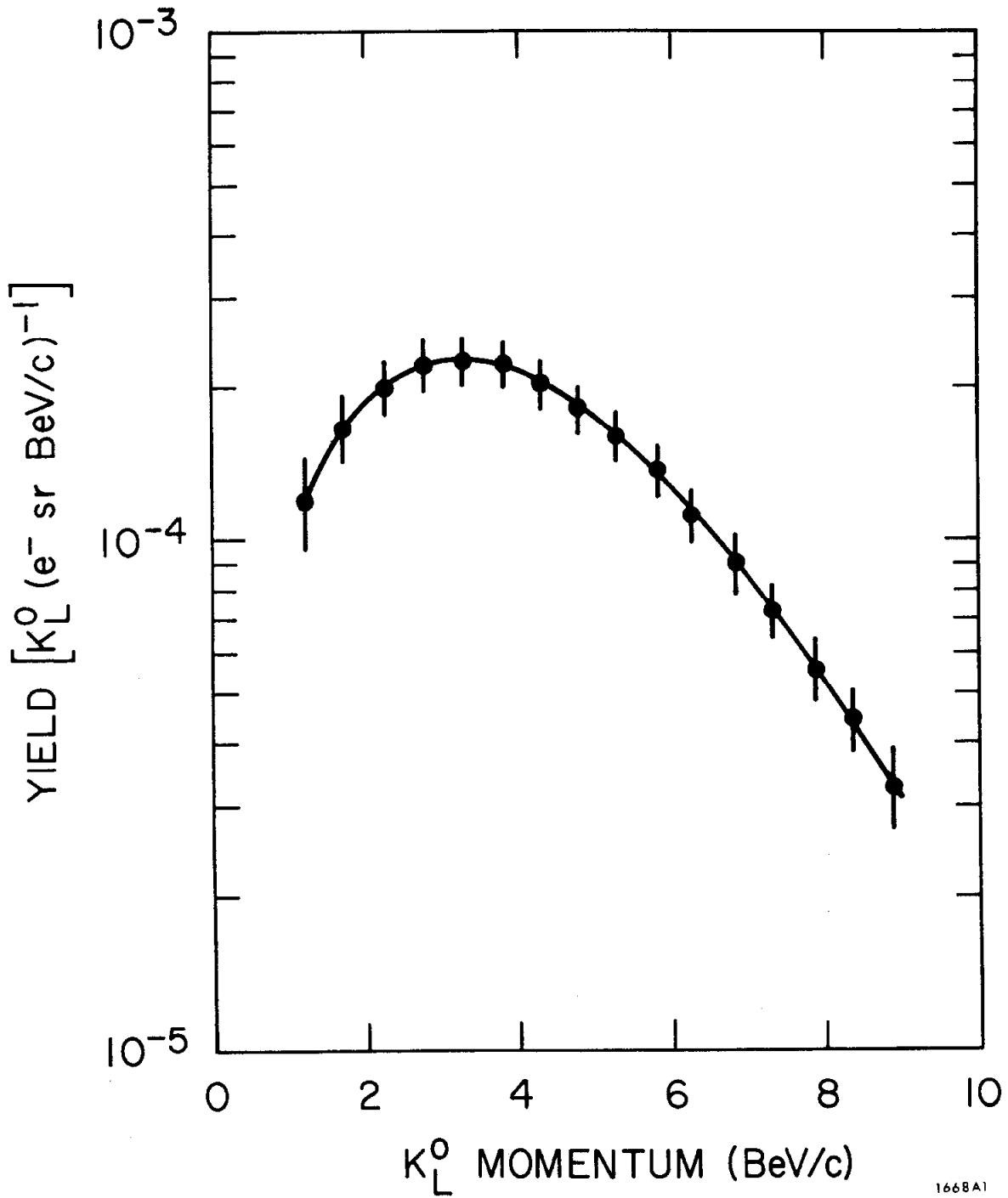
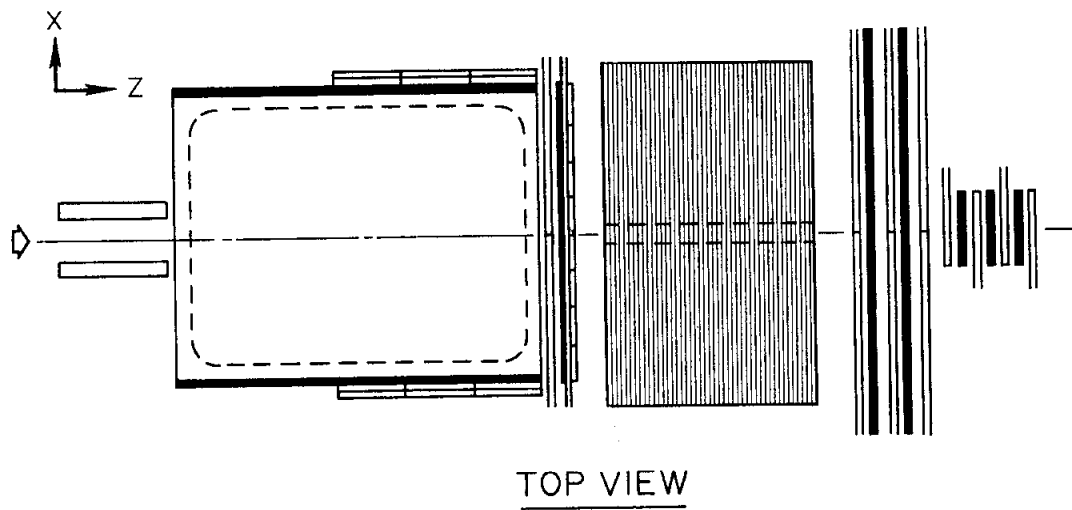
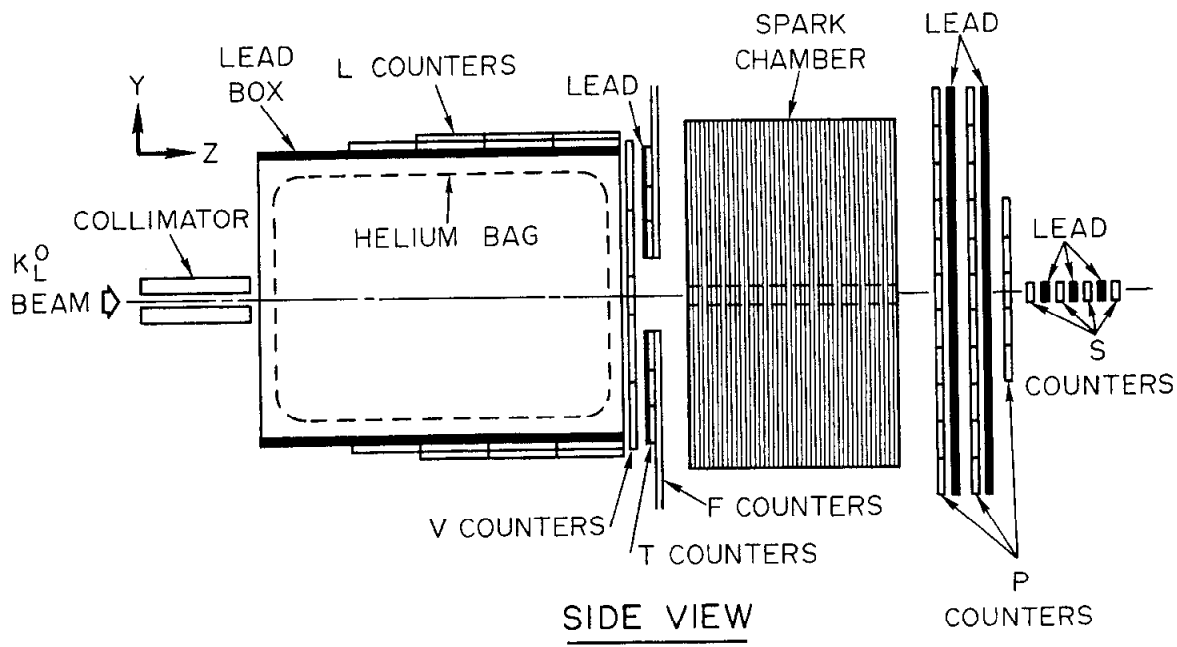


FIG. 2-- $K_L^0$  momentum spectrum at target.

The intensity of the beam was checked with a toroid current monitor and a Cerenkov cell upstream of the target, a secondary emission monitor looking at the target, and four counters (M's), placed just off the  $K_L^0$  beam upstream of the decay region, which detected charged decays. When the sweeping magnets were turned off the beam had a large component of fast muons.

The experimental apparatus is shown in Figs. 3 and 4. The beam entered the decay region through a final collimator whose slits were too large to effect the  $K_L$  beam. For part of the running this "collimator" was a 1/2 inch lead 1/2 inch scintillation counter sandwich. These "B" counters then defined the upstream edge of the decay region. This region was a helium filled box 47×47×48 inches in length, with four 1/2 inch (= .46 r. l.) lead walls. The helium was used to reduce the number of  $K_L$  interactions. The lead side walls were completely covered with scintillation counters. Gammas emitted at too great an angle to enter the spark chamber converted in the lead walls and were detected in these "L" counters. The downstream face of the decay box consisted of the "V" counters. They were used to detect charged particles from  $K_L^0$  decays or interactions in the region. This was followed by a 1/4 inch lead wall covering all but a 12 inch high slit about the beam line. It acted as a gamma converter. Behind this wall there were six horizontal "T" counters with phototubes at either end and sixteen vertical "F" counters with tubes on one end. Together they defined a matrix of 6×6 inch squares. Thus, the position of a converted gamma was roughly defined and the time at which it passed through a square could be determined from three different phototube signals.

A spark chamber with 63×63 inch cross section followed this counter bank. It had 40 gaps with 1/2 inch electrically independent copper-clad fiberglass-epoxy high voltage plates and 1/2 inch aluminum ground plates. The effective



1668A4

FIG. 3--Detection apparatus (collimation for first data run).

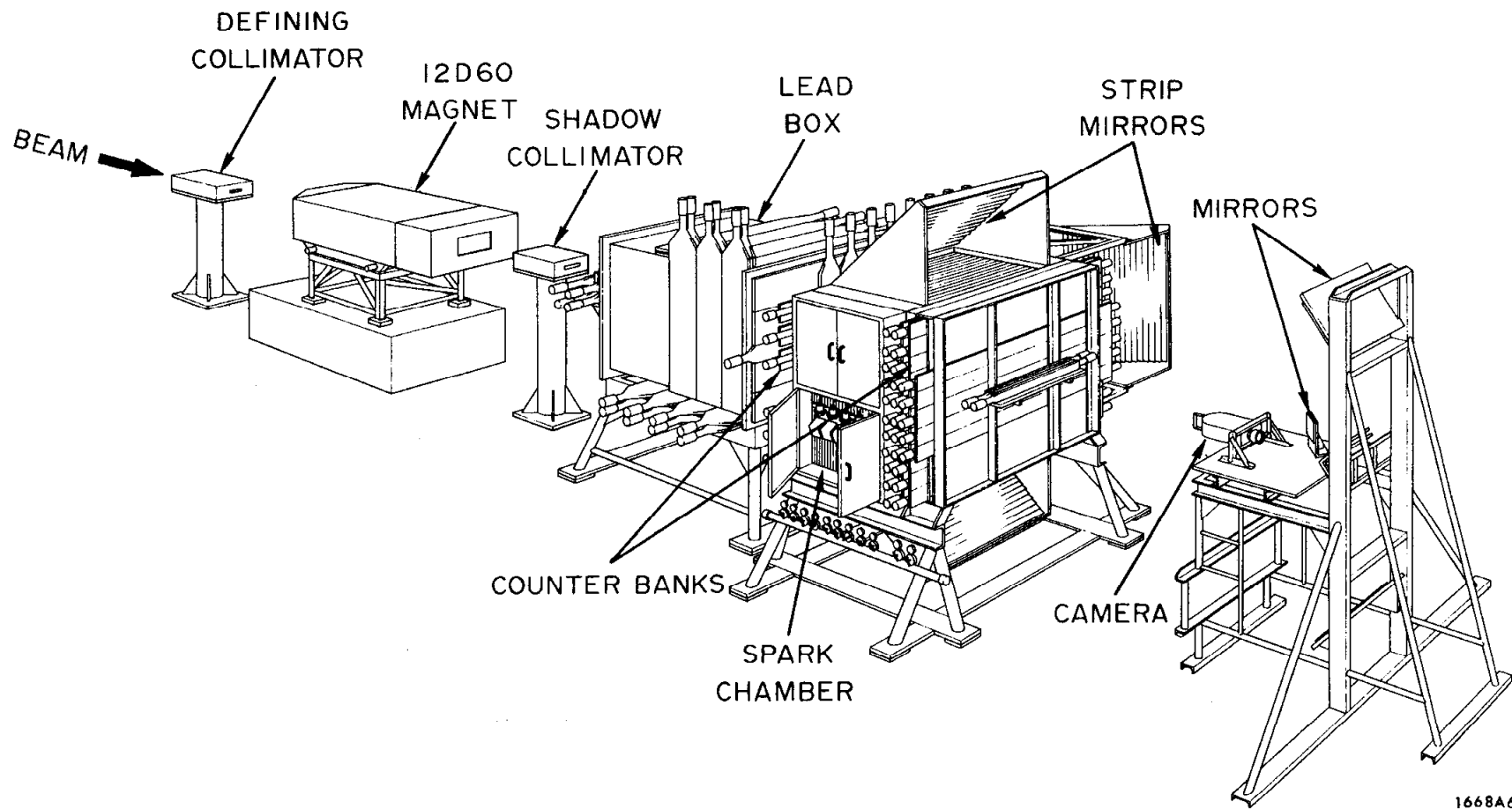


FIG. 4--Perspective view of detection apparatus (collimation for second data run).

length of the chamber was 4 radiation lengths. The independent high voltage plates helped improve the multitrack efficiency of the chamber. Also, the chamber gas was a mixture of neon-helium and isopropyl alcohol that maximized the multitrack efficiency. A 9X2 inch hole in the center of the chamber reduced interactions of the residual beam. The chambers were optically divided in the center and were viewed from the top, bottom and one side. This helped to reduce the number of apparently overlapping gamma showers on the film.

Since the length of the spark chamber was insufficient to completely absorb all of the showers, it was followed by two complete walls and one partial wall consisting of a 1/2 inch lead slab followed by scintillation counters. The pulse heights in these "P" counters measured the energy in the leftover gamma showers. There was also a group of four small "S" counters, separated from each other with 1/4 inch of lead, blocking the hole in the spark chamber. They were used to convert and detect gammas that came through this region.

A PDP-9 computer was used for on-line storage, histogramming, and display of data taken during the experiment. It had control over the high speed logic, camera and lights. It had the ability to test and calibrate the V, L, T, F and P counter banks by pulsing photodiodes imbedded in each of these counters. It recorded all of the counter information for each trigger on magnetic tape. In addition to the presence of a pulse in a counter, pulse heights for the T, F, S and P banks were available. Also, the timing of each T and F pulse with respect to the "cable" was measured. These functions were performed by specially designed, fast, 8 bit analog to digital converters.<sup>5</sup>

## OPERATION

The experiment had four different running modes. We first define the "normal" trigger designed to detect gamma decay modes ( $2\gamma$ ,  $2\pi^0$ ,  $3\pi^0$ ) and reject interactions and charged decays. The requirements were:

1. C - a timing reference pulse from the cable at the target.
2. T - both ends of at least one T must fire roughly simultaneously.
3. F - at least one F counter consistent with a struck T must fire.

Requirements 1, 2 and 3 allow sufficient information for the timing measurement.

4.  $2P = P\text{-black and } P\text{-white}$  - consider the P bank as a  $2 \times 11$  checker-board, at least one black and one white counter must fire. This requirement was satisfied by nearly all showers which naturally spread into a cone that would cover neighboring P-counters. It is not met by single charged particles, background pions and muons for example.
5.  $\bar{V}$  - no pulse in any of the V's. Such a pulse would indicate a charged particle leaving the decay volume.
6.  $\bar{B}$  - no pulse in any of the B's. Such a pulse would indicate an event upstream of the decay region.

The L and S counters were not part of the trigger and were simply recorded for each event.

During normal running every tenth event was taken under a "monitor" trigger. This trigger was biased toward charged decays, namely,  $\pi\mu\nu_\mu$ ,  $\pi e\nu_e$  and  $\pi^+\pi^-\pi^0$ . The requirements were:

1.  $C \cdot 2(TF) \cdot \bar{B}$  - with elements as defined above.
2.  $2V$  - two out of the three pairs of adjacent V's must fire.

Charged and neutral decay rates could then be compared since the time between events was known.

To test our understanding of the apparatus, we ran for a while with 8 inches of copper regenerator in the decay box. The regenerator could be placed anywhere in a region between 40 and 70 inches upstream of the spark chamber. An additional "A" counter was placed immediately in back of the regenerator to detect charged products of interactions. The regenerator trigger was  $(C \cdot (TF) \cdot 2P \cdot \bar{V} \cdot \bar{B}) \cdot \bar{A}$  and the monitor was  $(C \cdot 2(TF) \cdot 2V \cdot \bar{B}) \cdot \bar{A}$ . During this running either trigger was allowed to define an event. The intensity of the beam had to be reduced in this mode because the large number of interactions in the regenerator increased the accidental rate.

As a timing calibration we periodically ran muons through the apparatus, with the spark chamber and sweeping magnets turned off. The trigger was  $C \cdot (TF) \cdot P \cdot V$ . We could then measure the arrival time of the fast muons with respect to the cable pulse.

#### DATA REDUCTION

Approximately 200,000 pictures were used in the analysis. The film was scanned by physicists. Approximately 70% of the pictures were either blank, had single mesons, or contained kaon interactions in the chamber. Valid neutral decays were classified according to the number of visible showers. Four gamma events that obviously violated momentum conservation or did not have an obvious trigger were dropped at this stage since they clearly were not legitimate  $2\pi^0$  events. Monitor events were classified according to decay mode whenever possible. Detailed measurement instructions were generated by the scanners indicating the initial conversion points, the extent of each shower or track and the points to be used for the direction determination. Events were

measured on an image plane digitizer. The reconstruction error was 0.15 inches in the chamber. A second independent scan of the regenerator film gave an overlap of about 85% for the number of four gamma decays. The quality of the missing 15% is unclear, ranging from unanalyzable to normal. Thus the four gamma scanning efficiency is between 85 and 100%.

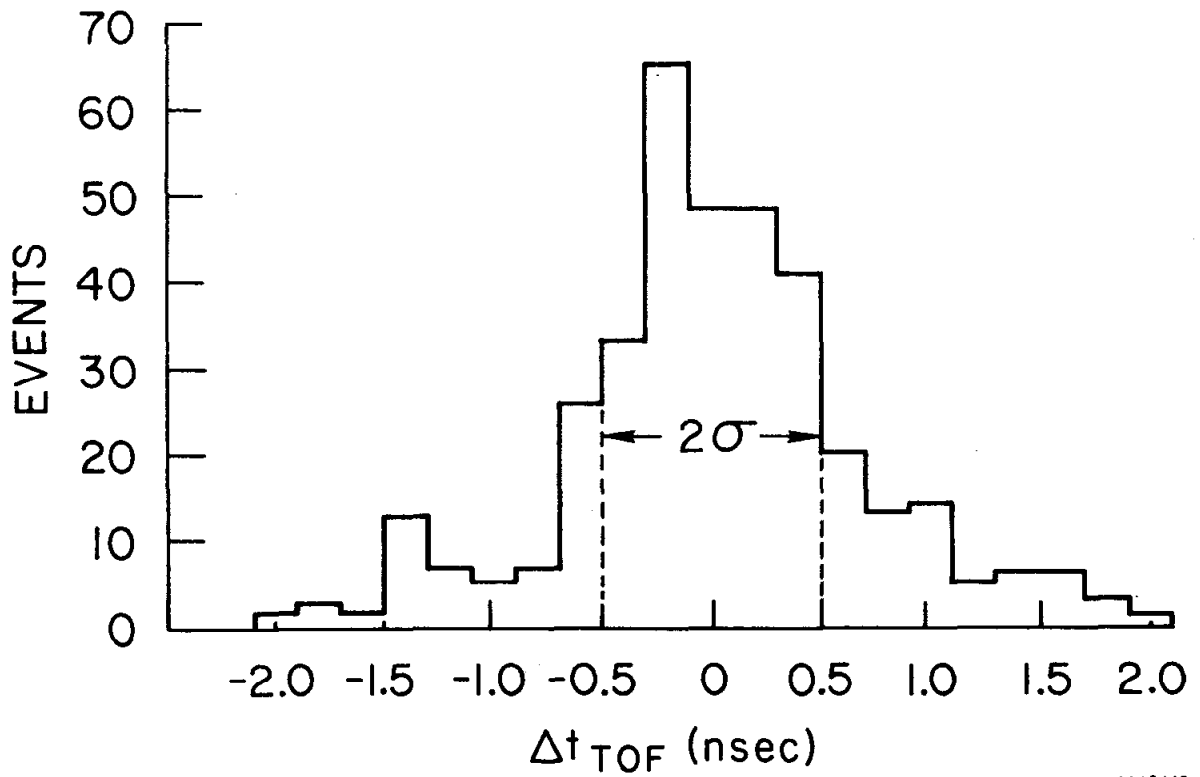
The measured data was used to reconstruct each track in real space and the direction cosines of each were obtained by a least squares method. A weight was assigned to each track depending on the single point reconstruction error, the number of points used to determine the direction, their spatial extent, and the amount of material the track had passed through which would cause multiple scattering. Weights for conversion points were determined by reconstruction accuracy and the same type of multiple scattering correction. Also the range of each track, in gaps, was retained. The fitted tracks were then combined to obtain a best fit for a single vertex constrained to lie in the collimated decay region. Final, more accurate, direction cosines were formed using the fitted vertex and measured conversion points. Vertex errors in the beam direction were typically 10% of the distance from vertex to the front of the spark chambers.

Raw timing data from the T and F banks could now be used to get the time-of-flight from the target and thus the momentum of the incoming particle, assuming it to be a  $K^0$ . The light pulser tests gave a scale calibration of the ADC time outputs. The muon runs gave the zero point corresponding to particles traveling with speed  $c$ . This is not an exact determination because of uncertainties in muon flight paths. Corrections to these times were made for the distance from the geometric vertex to the TF square hit. Also, a pulse height slewing correction was made to eliminate the effect of the discriminator



threshold that determined the time. The time calculation was first applied to all possible triplets, two sides of a T counter and an F. If that failed to yield any consistent results, timing was attempted on doublets after eliminating the earliest time. This was done because if two gammas hit the same T counter but different F counters, then for each gamma the F counter and one end of the T yield the proper time while the other end will be earlier. The failure rate of the timing algorithm was about 3%. The error in this algorithm can be estimated by comparing times between several valid triplets of a single event (Fig. 5). This distribution has a variance of about 0.5 nanosecond. Thus the timing error for a single counter is  $0.3 = 0.5 / \sqrt{2}$  nanoseconds. Such an error determines the momentum of a 3 GeV/c  $K_L^0$  to 8%. This algorithm did not completely determine the time. A final additive constant was gotten by demanding agreement between the position of the leading edge in the time-of-flight histogram (Fig. 6) and the Monte Carlo prediction. This was done for all 3-6 gamma events. This calibration relies on the high energy  $K^0$  spectrum and not on the details of the Monte Carlo.

The pulse heights from the P, T and F counters had to be associated with the proper tracks observed in the spark chamber. T and F pulse heights were assigned to any track that extrapolated to a point within them. If there was more than one track the pulse height was equally divided. For P counters the spread and length of the shower had to be considered. Therefore pulse heights were assigned to any track that extrapolated to a point within 5 inches of the counter. In cases of conflict where one track's shower appeared to end more than two radiation lengths earlier than those of the others, that track was eliminated. Pulse height was then divided equally among the remaining showers.



1668A13

FIG. 5--Difference between corrected triplet times for good 3-6γ events from first data run.

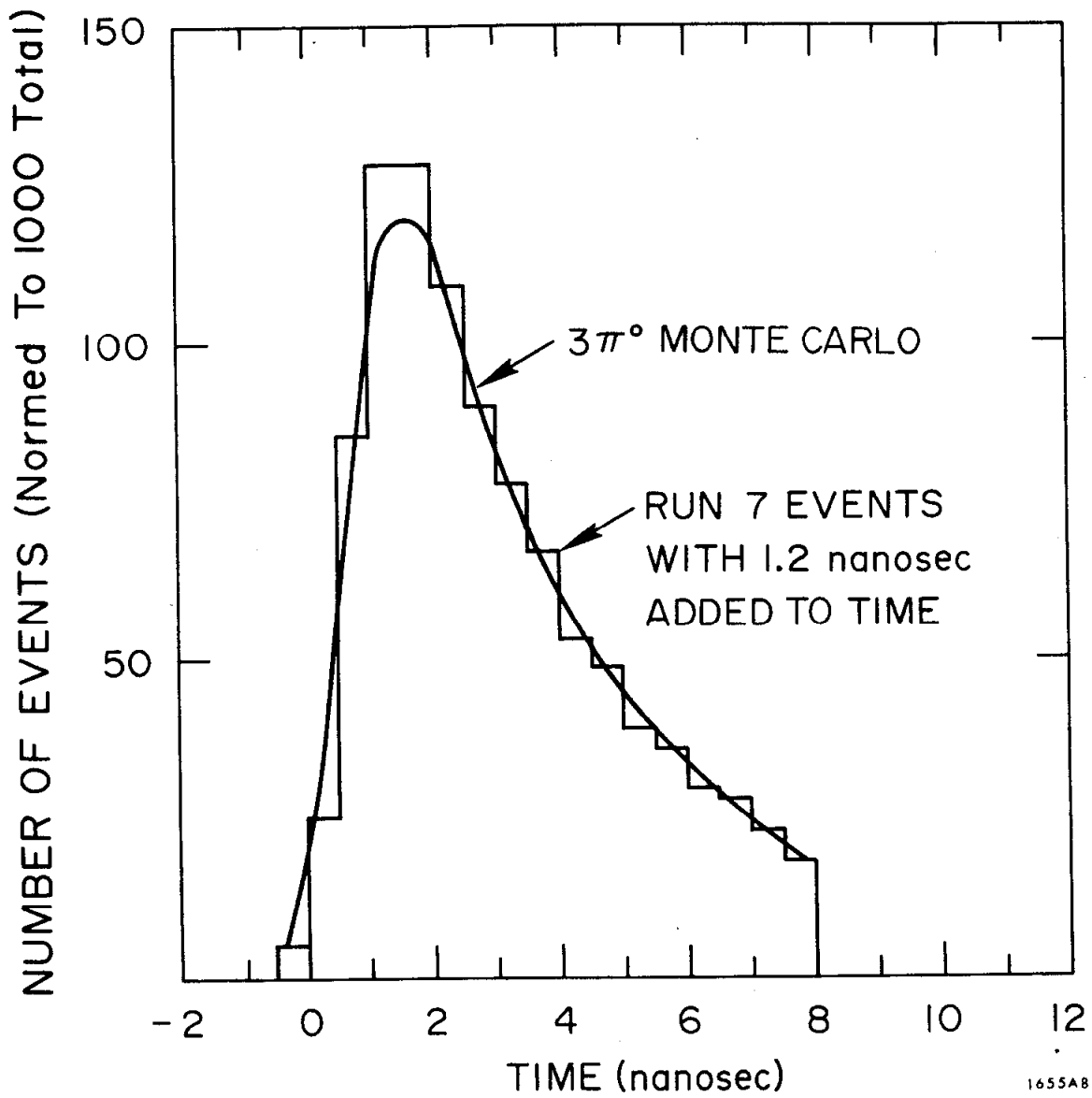


FIG. 6--Time-of-flight for 3-6 $\gamma$  events

The neutral decays were divided into two parts. "Unlatched" events are clean events with no indications of missing showers. An event was considered to be "latched" if any of the following occurred; an L counter had fired, the S counters indicated a missing shower, there was a valid triplet in the TF bank without an associated track, or there was a large amount of unassigned pulse height in the P counters.

#### NORMALIZATION

In order to obtain the branching ratio we needed to know the number of three pion decays in the decay region. This could be determined from the observed number of  $\geq 3$  gamma events and from the efficiency for seeing such events as predicted by a Monte Carlo calculation. The observed number of multigamma decays is given in Table 1. It was found that 17% of the six gamma events had an additional L counter, which we assume to be accidental. Examination of these events showed no other difference compared to the unlatched events. We therefore assumed an accidental latched rate of 17% for all of the gamma decays. The  $K_L \rightarrow 3\pi^0$  Monte Carlo was done in the following way. The momentum of the K and its decay point were distributed according to the measured K spectrum and the beam position. The  $\pi^0$ 's were distributed isotropically in the center of mass, allowed to decay, and the gammas were transformed to the laboratory frame. The detection efficiency was a combination of geometric efficiency, gamma conversion probability and scanning criteria. The calculation of gamma conversion probability based on the lead and spark chamber composition agreed with the observed results. The resulting detection efficiency is given in Table 1.

The normalization calculation could be checked by using the observed number of leptonic decays seen during the monitor trigger, the Monte Carlo detection

TABLE 1

Normalization

	$K_L^0 \rightarrow 3\pi^0 (>3\gamma \text{ seen})$	$K_L^0 \rightarrow \pi\mu\nu_\mu$	$K_L^0 \rightarrow \pi e\nu_e$
Number of scanned events	38,600	951	378
Number unlatched, with valid triplets and satisfying all cuts	30,700	550	279
Fraction of total run	100%	3.6%	3.6%
Average triggering efficiency	$0.36 \pm 0.04$	$0.13 \pm 0.01$	$0.05 \pm 0.005$
Number of decays	$86000 \pm 8000$	$115000 \pm 12000$	$153000 \pm 17000$
$\Gamma(\text{decay})/\Gamma(K_L^0 \rightarrow \text{all})^7$	$0.215 \pm 0.007$	$0.268 \pm 0.007$	$0.388 \pm 0.008$
Number of $K_L^0$	$399000 \pm 39000$	$429000 \pm 46000$	$393000 \pm 45000$
<hr/>			
Average Number of $K_L^0$ unlatched	$407000 \pm 25000$		
Average Number of $K_L^0 \rightarrow 3\pi^0$ unlatched	$88000 \pm 5000$		

efficiencies for these events, and the known branching ratios for these modes. The monitor event sample was restricted in the following ways. To give a better direction measurement the apparent "pion" must not interact before the fifth gap of the chamber. For identification purposes, the "muon" must travel through the lead T and F counters and the entire spark chamber. This corresponds to a minimum range of  $125 \text{ gm/cm}^2$  and a minimum muon energy of 0.35 GeV. Also, for identification and to insure a good direction measurement, the "electrons" were required to miss the lead in front of the T and F counters. The Monte Carlo for the leptonic decay modes starts with a decay in the center of mass weighted using the experimental  $K_{e3}$  form factors.<sup>6</sup> We then distribute the events according to the measured K spectrum and the beam position. The final efficiency is a combination of the geometrical efficiency for the event to produce a trigger and the probability of its satisfying the scanning criteria. A correction is made for the accidental latch rate. These results are given in Table 1. It can be seen that the three normalizations are consistent and give the average results shown.

#### REGENERATOR ANALYSIS

There are about 900  $2\pi^0$  candidates in the regenerator running. A modified SQUAW fitting program was used to test the  $2\pi^0$  hypothesis. A preliminary track energy formula was obtained from the measured six gamma events. We used a linear form  $E = aT + bN + cP \sqrt{1 + L}$  where T is the T and F counter pulse height, N is the number of gaps traversed by the shower, P is the P counter pulse height, and L is the distance in radiation lengths traveled by the gamma in the spark chamber before converting. The reason for the  $\sqrt{1 + L}$  factor is that since the apparatus does not completely absorb the higher energy showers, more energy is lost for showers which convert late in the chamber.

The three coefficients were obtained by minimizing the chi square

$$\chi^2 = \sum \left( \frac{E_T - E_M}{E_T + E_M} \right)^2 \quad \text{where } E_M = \sum_{i=1}^6 E_i. \quad E_T \text{ is the kaon energy determined}$$

from the time and the summation is over all these  $6\gamma$  events. The unlatched events that were within an 80 MeV  $K_L^0$  mass peak were then used to generate a final energy formula. Also a group of apparently valid  $2\gamma$  events were added to the sample to increase the statistics for higher energy showers. The final formula had the form

$$E_M = aT + bN + cNT + d(1 + eL) \left( 1 - \frac{X}{150} \right) (1.5 P_I + P_0)$$

where T, L and N are as before. X is the distance of the center of the shower from the center of the P bank and simulated a loss of efficiency at the end of the counter away from the photomultiplier.  $P_I$  and  $P_0$  are the P pulse heights for the three and two sandwich areas of the P bank and were therefore weighted differently. The five coefficients were obtained by minimizing

$$\chi^2 = \sum \left( \frac{E_{Fi} - E_{Mi}}{E_{Mi}^2} \right)^2$$

where  $E_F$  is the energy of each gamma given by the SQUAW fit, or the  $2\gamma$  analysis, and the sum is over all tracks of the "good"  $4\gamma$  and  $2\gamma$  events. Other terms were tried in the energy formula but showed no appreciable improvement. In particular, replacing the number of gaps with the number of sparks for each track was to no great advantage. This scheme gave a gamma energy determination to about 40%.

Using the final energy formula and after vertex and kinematic cuts the resulting regenerator mass plots are shown in Fig. 7 for unlatched and latched type events. The peak in the unlatched distribution was used in lines 1 and 2 of

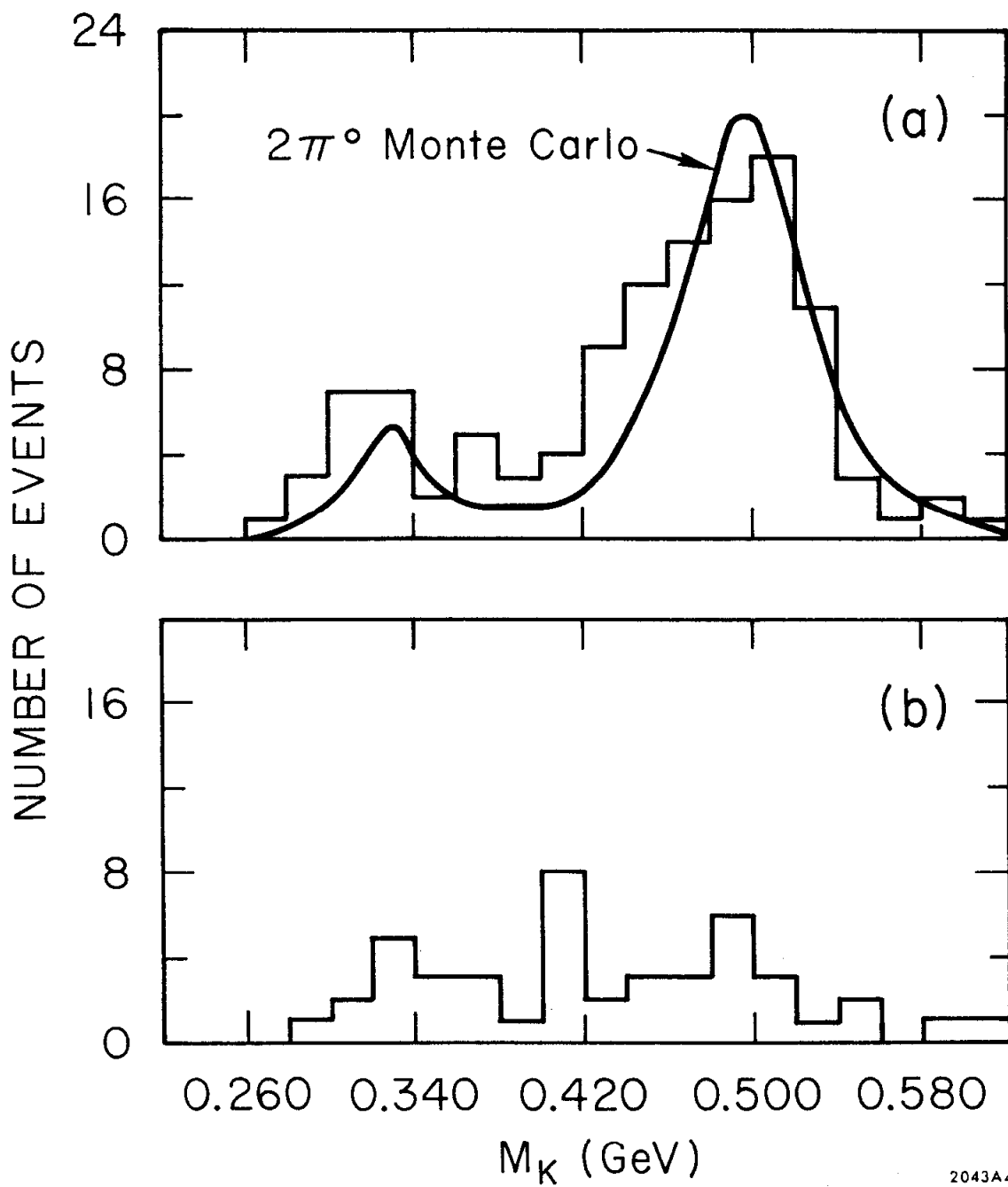


FIG. 7-- $K_L^0$  mass for 4 $\gamma$  regenerator, (a) unlatched (b) latched.



Table 2 to calculate the number of regenerated  $K_S^0$ . We could also use the direction and momentum information, in the way described in the next section, to calculate the angle between the two pions in the center of mass (Figs. 8 and 9). This gives lines 3, 4 and 5 of Table 2.

#### PI-PI OPENING ANGLE ANALYSIS

The final selection of good  $2\pi^0$  events was done by separating the signal from the background in histograms of the cosine of the center of mass angle between the two  $\pi^0$ 's. We used this method, rather than the SQUAW fitting procedure, because we were unsure as to the effect on  $K^0$  mass plots of the large uncertainty in gamma energies. This is illustrated by the slewing of the regenerator mass peak (Fig. 7), which cannot be mimicked by the Monte Carlo. Also the SQUAW procedure did not give us separation between signal and  $3\pi^0$  background in the mass plot. The opening angle analysis avoided these problems by relying more on the ratios of gamma energies. The analysis was applied to  $4\gamma$  events with K momentum between 1.8 and 5.8 GeV/c, vertex in the decay region, and measured energy of each track greater than 75 MeV.

We first transformed each track to the center of mass system using the comparatively accurate determination of the K momentum. If we assumed  $K_L^0 \rightarrow 2\pi^0$  there were three possible pairings of the four gamma tracks. The kinematics gave us the probability distribution for the center of mass angle between two gammas of a pair. This must be greater than  $65^\circ$  and falls rapidly for larger angles. We calculated the relative likelihoods of each of the three pairings and dropped all but the best one. We then calculated  $\cos \theta_{\pi\pi}$ , the angle between the two pions in the center of mass. Looking at a plot of this quantity for regenerator  $4\gamma$  (Fig. 8) events we clearly have a peak at  $\cos \theta_{\pi\pi} = -1$ .

TABLE 2  
Regenerator  $2\pi^0$  Analysis

	Number of Events	M. C. Efficiency	Total $K_S^0 \rightarrow 2\pi^0$ Unlatched
1. SQUAW 40 MeV Peak	$34 \pm 6$	.32	$106 \pm 19$
2. SQUAW 60 MeV Peak	$47 \pm 7$	.41	$115 \pm 17$
3. $\cos \theta_{\pi\pi}$ Extrapolation with Kinematical cuts	$30 \pm 6.8$	.25	$120 \pm 30$
4. $\cos \theta_{\pi\pi} < -0.85$ with Kinematical cuts	$37 \pm 6$	.36	$103 \pm 17$
5. $\cos \theta_{\pi\pi}$ Extrapolation	$37 \pm 15.4$	.34	$109 \pm 45$
6. Calculation from Number of $K_L^0$ and MC Regenerator Simulation			$129 \pm 20$

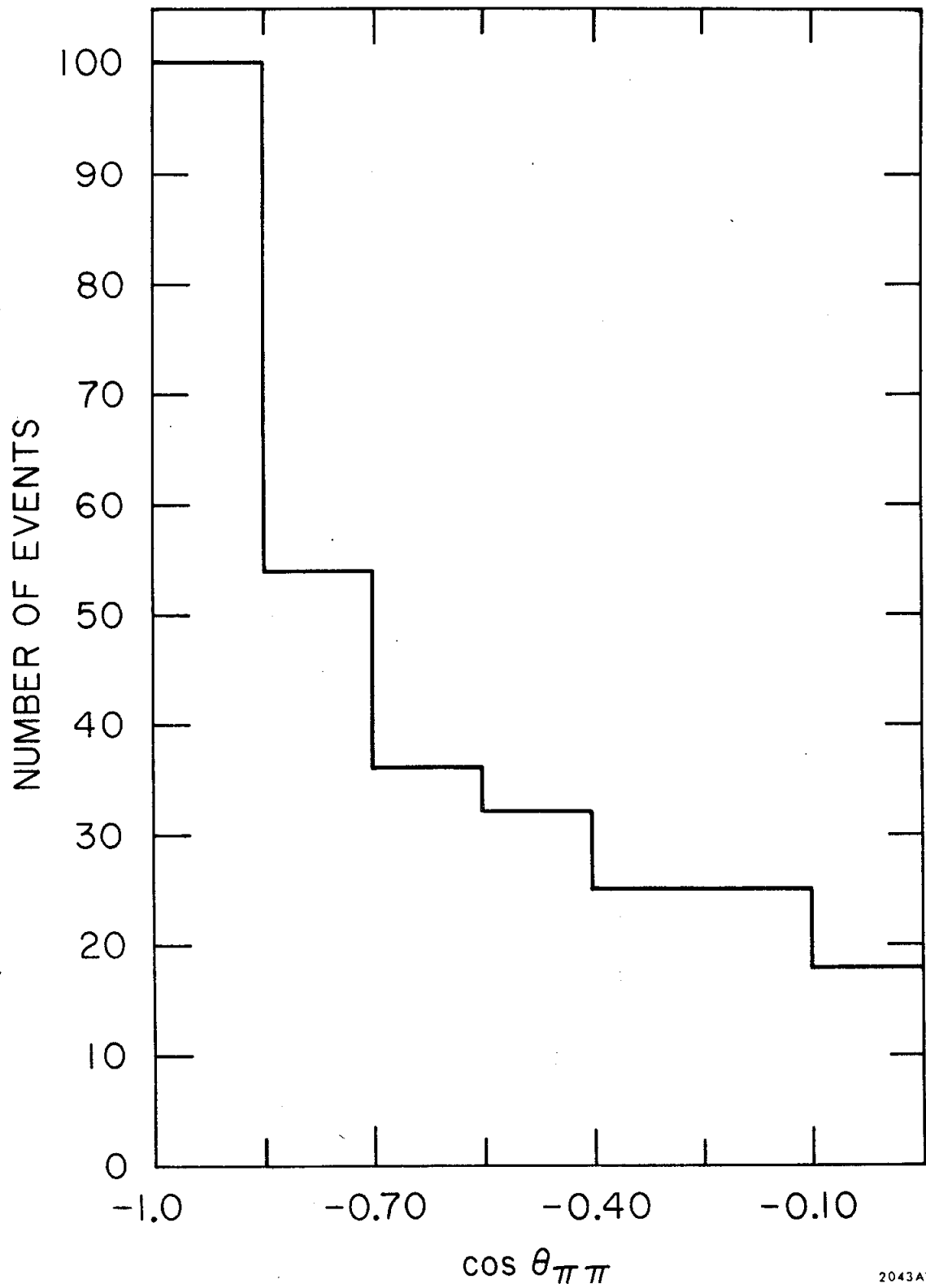


FIG. 8-- $\cos \theta_{\pi\pi}$  for  $4\gamma$  regenerator, unlatched.

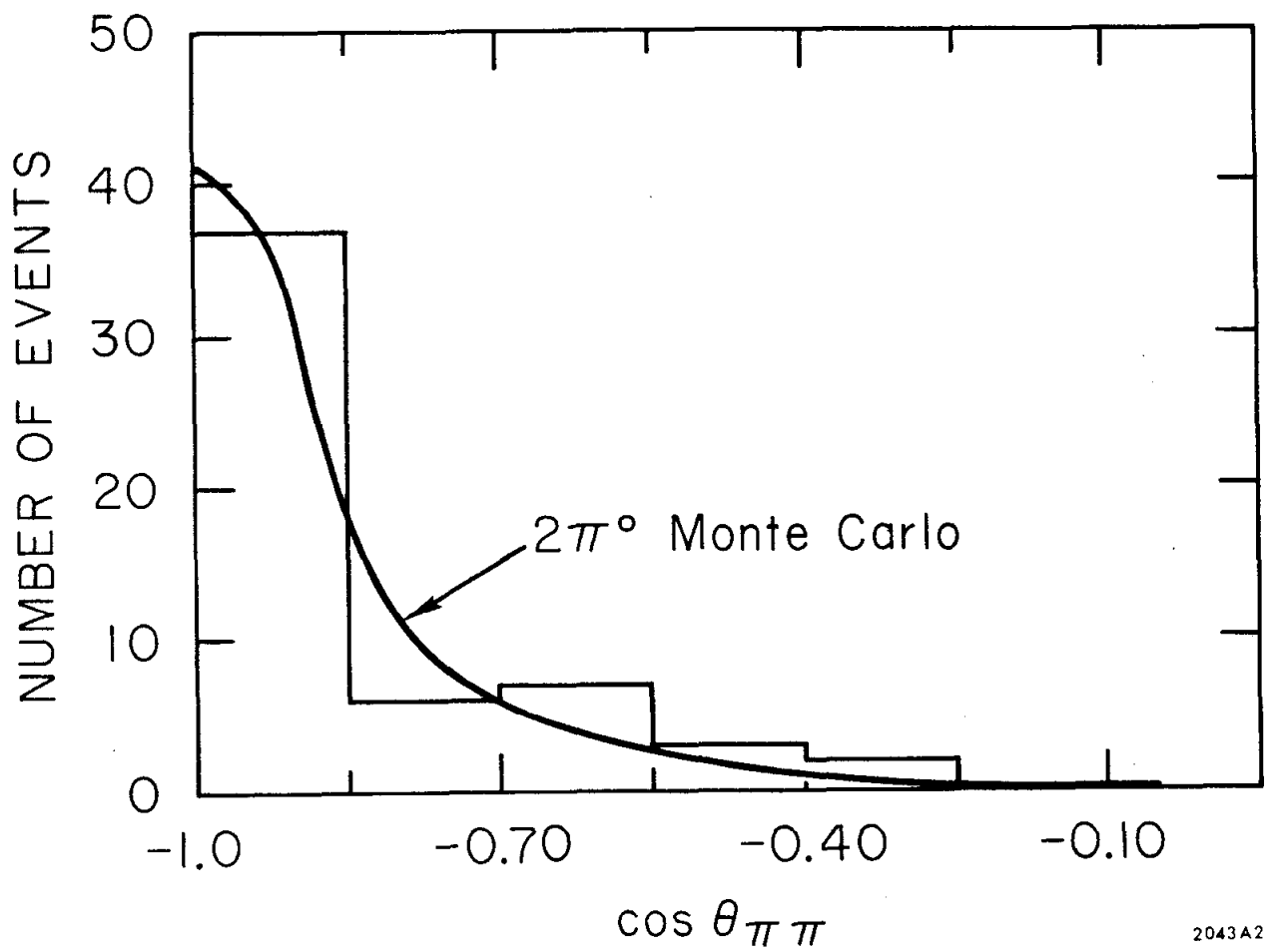


FIG. 9-- $\cos \theta_{\pi\pi}$  for  $4\gamma$  regenerator with kinematical cuts, unlatched.

However, we have not sufficiently reduced the  $3\pi^0$  background in the normal running case (Fig. 10).

To further reduce the  $3\pi^0$  background we imposed additional kinematical cuts. Following Gaillard et al.,<sup>6</sup> we calculated the  $\pi^0$  energy corresponding to two gammas in a way that depended only on the ratio of the gamma energies. The laboratory  $\pi^0$  energy was given by

$$E_i = \frac{m_\pi(1 + \epsilon_{1i}/\epsilon_{2i})}{\sqrt{2(\epsilon_{1i}/\epsilon_{2i})(1 - \cos \theta_{12})}}$$

where  $\epsilon_{1i}$  and  $\epsilon_{2i}$  are the gamma energies and  $\theta_{12}$  is the angle between the two gammas we assume came from this  $\pi^0$ . We then calculated

$$\chi^2 = \left( \frac{E_1 - \epsilon_{11} - \epsilon_{21}}{E_1} \right)^2 + \left( \frac{E_2 - \epsilon_{12} - \epsilon_{22}}{E_2} \right)^2$$

$$m_k = \sqrt{(E_1 + E_2)^2 - (p_1 + p_2)^2} \quad |p_i|^2 = E_i^2 - m_\pi^2$$

$$\Delta = |E_{1cm} - E_{2cm}|$$

For a true  $K_L^0 \rightarrow 2\pi^0$ ,  $m_k = 0.497$  GeV and  $\chi^2 = \Delta = 0$ . Making cuts on these quantities should eliminate background events. With  $\chi^2 < 0.8$ ,  $0.45 \text{ GeV} < m_k < 0.55$  GeV and  $\Delta < 0.075$  GeV we obtained Fig. 11 for unlatched and latched  $4\gamma$  events from the normal running and Fig. 9 for the regenerator events.

The regenerator shows a peaking as  $\cos \theta_{\pi\pi} \rightarrow -1$  in both cases (Figs. 8 and 9). In the case where we have imposed cuts the background appeared to be negligible, therefore we used the events in the first bin,  $\cos \theta_{\pi\pi} < -0.85$ , as a measure of the signal (Table 2, line 4). This technique could not be used for the normal running  $4\gamma$  events because of the background.

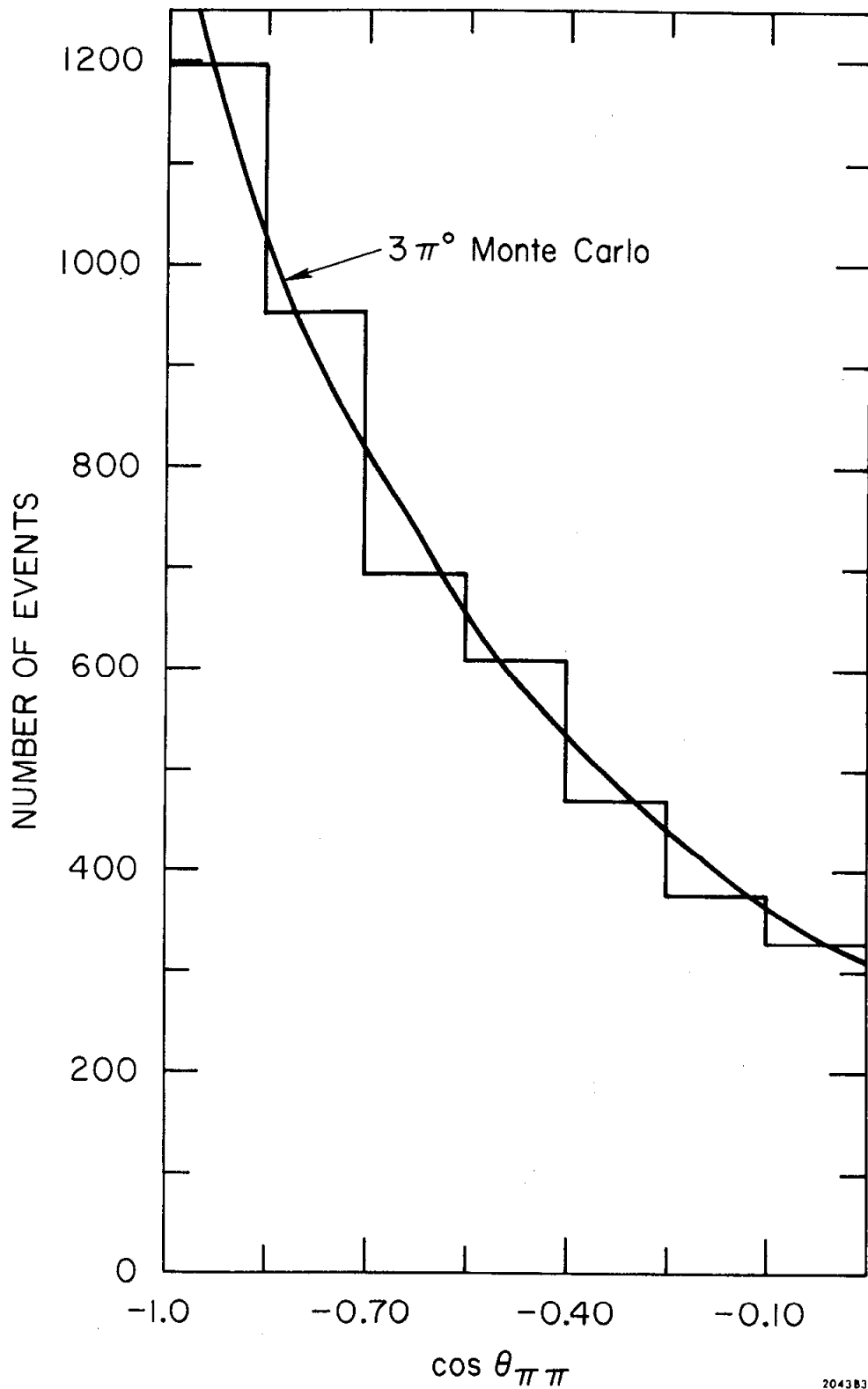


FIG. 10-- $\cos \theta_{\pi\pi}$  for normal running  $4\gamma$ , latched and unlatched.

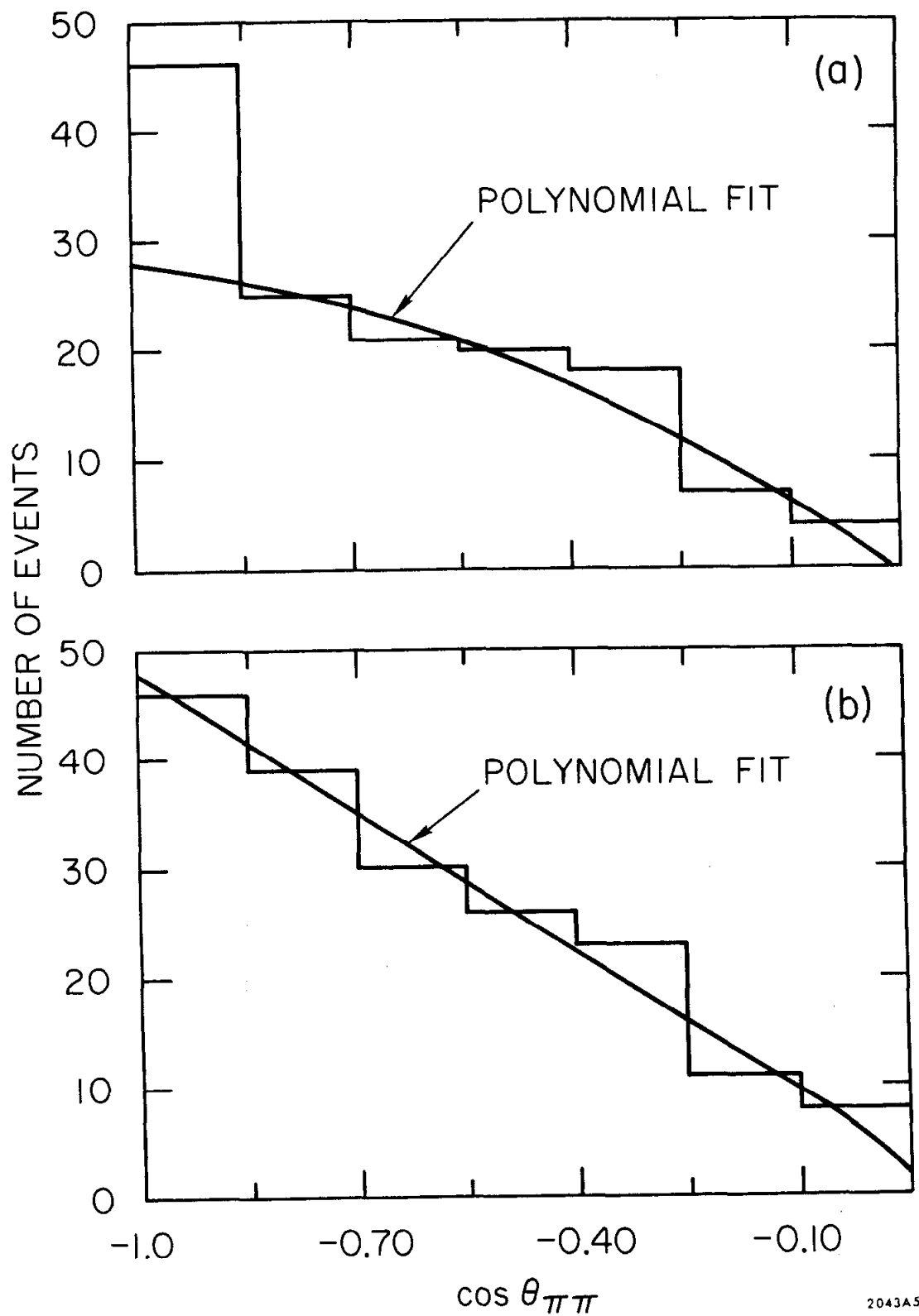


FIG. 11-- $\cos \theta_{\pi\pi}$  for normal running  $4\gamma$  with kinematical cuts  
 (a) unlatched (b) latched.

2043A5

For both the normal running and the regenerator, we extracted the number of  $2\pi^0$  events in the first bin by performing a background subtraction. We assumed that the background in the first bin could be extrapolated from the higher bins using a second order polynomial in  $\cos\theta_{\pi\pi}$ . The coefficients of this polynomial were determined by a least squares fit to the higher bins. This assumption was not checked for the regenerator events since we did not have a model for the background, which was small. The application of this polynomial extrapolation procedure to the regenerator events gave lines 3 and 5 of Table 2.

Generation of the  $2\pi^0$  Monte Carlo events is identical to the  $3\pi^0$  case previously described. To obtain analysis efficiencies we include errors and distributions in the tracks due to; scattering in the lead in front of the TF bank, geometric reconstruction, multiple scattering in the spark chamber, conversion depths in the chamber, useful track lengths and the gamma energy determination. The resulting simulated  $2\pi^0$  events were used in the SQUAW program and led to the Monte Carlo analysis efficiencies shown in lines 1 and 2 of Table 2. Running the same events through the opening angle analysis gave the efficiencies shown in lines 3, 4 and 5 of that table. The agreement between the  $2\pi^0$  M. C. and the regenerator events is shown in the opening angle plot of Fig. 9. Using the measured number of  $K_L^0$  in the regenerator run, the experimentally determined regeneration parameters for copper and the Monte Carlo detection efficiency for  $2\pi^0$  events we got another determination of the number of  $K_S^0 \rightarrow 2\pi^0$  (line 6, Table 2). We see that these six determinations of the number of unlatched  $K_S^0 \rightarrow 2\pi^0$  in the regenerator runs are in agreement.

A large sample of  $3\pi^0$  Monte Carlo events were run through the opening angle analysis. Agreement with the experimental data without kinematical cuts is shown by Fig. 10. Reasonable agreement was maintained after these cuts



were imposed. Exact agreement was not crucial since the principal assumption was the smoothness of the background and not its precise shape. The same polynomial extrapolation procedure was used to obtain the number of good  $2\pi^0$  events in the normal running. The smoothness assumption was checked by looking at the latched events with kinematical cuts, Fig. 11. b, which showed no signal above the extrapolated background. It was also checked by applying the procedure to separate a small number of  $2\pi^0$  Monte Carlo events, the signal, from a large sample of  $3\pi^0$  Monte Carlo events, the background. It was found that the extrapolation procedure always gave slightly fewer events than required by the Monte Carlo. We compensated for this by applying a negative correction to the background, proportional to the number of events in the higher bins of the  $\cos\theta_{\pi\pi}$  plot. The resulting procedure always yielded the correct fraction of  $2\pi^0$  events in the mixture, over a wide range of such mixtures. Furthermore, these results were insensitive to the exact form of the gamma ray errors.

## RESULTS

Applying the extrapolation procedure and using the Monte Carlo analysis efficiency gives us the number of detectable  $K_L^0$ . We get  $13 \pm 10$  events in Fig. 11. a. , an analysis efficiency of  $0.33 \pm 0.03$  and a scanning efficiency of 85%. This gives  $46 \pm 36$  detectable events. Combining this with a  $2\pi^0$  detection efficiency of 16% and the  $K_L^0$  flux we get

$$\Gamma(K_L \rightarrow 2\pi^0) / \Gamma(K_L \rightarrow 3\pi^0) = \frac{278 \pm 222}{88000 \pm 5000} = 3.2 \pm 2.5 \times 10^{-3}$$

$$|\eta_{00}|^2 = 3.6 \pm 2.9 \times 10^{-6}$$

This result is in agreement with the world average<sup>7</sup>

$$|\eta_{00}|^2 = 4.9 \pm 1.0 \times 10^{-6}$$

The two main reasons for the large error are the small number of events and the large uncertainty in the gamma momentum determination.

## REFERENCES

1. A detailed review article is T. D. Lee, C. S. Wu, *Annu. Rev. Nucl. Sci.* 16, 511 (1966).
2. J. Enstrom, *et al.*, *Phys. Rev. D* (to be published) or SLAC-PUB-909 (1971). J. Enstrom, Report No. SLAC-125 (1970).
3. R. B. Neal, The Stanford Two-Mile Accelerator (W. A. Benjamin, Inc., New York, 1968).
4. A. D. Brody, *et al.*, *Phys. Rev. Letters* 22, 966 (1969).
5. D. Porat and K. Hense, *Nucl. Instr. Methods* 67, 229 (1969).
6. Particle Data Group, "Review of Particle Properties", *Rev. Mod. Phys.* 43, S1 (1971).
7. J. M. Gaillard, *et al.*, *Nuovo Cimento* 59A, 453 (1969).